

Importance of an N-Terminal Extension in Ribonuclease HII from *Bacillus stearothermophilus* for Substrate Binding

AYUMU MUROYA,¹ RIKITA NAKANO,¹ NAOTO OHTANI,¹ MITSURU HARUKI,¹
MASAAKI MORIKAWA,¹ AND SHIGENORI KANAYA^{1*}

Department of Material and Life Science, Graduate School of Engineering, Osaka University,
2-1 Yamadaoka, Suita, Osaka 565-0871, Japan¹

Received 29 October 2001/Accepted 20 November 2001

The gene encoding ribonuclease HII from *Bacillus stearothermophilus* was cloned and expressed in *Escherichia coli*. The overproduced protein, *Bst*-RNase HII, was purified and biochemically characterized. *Bst*-RNase HII, which consists of 259 amino acid residues, showed the highest amino acid sequence identity (50.2%) to *Bacillus subtilis* RNase HII. Like *B. subtilis* RNase HII, it exhibited Mn²⁺-dependent RNase H activity. It was, however, more thermostable than *B. subtilis* RNase HII. When the *Bst*-RNase HII amino acid sequence is compared with that of *Thermococcus kodakaraensis* RNase HII, to which it shows 29.8% identity, 30 residues are observed to be truncated from the C-terminus and there is an extension of 71 residues at the N-terminus. The C-terminal truncation results in the loss of the α 9 helix, which is rich in basic amino acid residues and is therefore important for substrate binding. A truncated protein, Δ 59-*Bst*-RNase HII, in which most of the N-terminal extension was removed, completely lost its RNase H activity. Surface plasmon resonance analysis indicated that this truncated protein did not bind to the substrate. These results suggest that the N-terminal extension of *Bst*-RNase HII is important for substrate binding. Because *B. subtilis* RNase HII has an N-terminal extension of the same length and these extensions contain a region in which basic amino acid residues are clustered, the *Bacillus* enzymes may represent a novel type of RNase H which possesses a substrate-binding domain at the N-terminus.

[Key words: RNase H, *Bacillus stearothermophilus*, gene cloning, N-terminal truncation, substrate binding]

Ribonuclease H (RNase H) cleaves the P-O3' bond of the RNA portion of DNA/RNA hybrids (1). The enzyme, which is universally present in diverse organisms, is thought to be involved in the removal of RNA primers from Okazaki fragments and of R-loops associated with transcription, but its physiological functions are not yet fully understood (2). Based on differences in their amino acid sequences, RNases H are classified into two major families, Type 1 and Type 2 (3, 4). The Type 1 enzymes can be further divided into bacterial RNases HI, eukaryotic RNases HI, and the RNase H domains of reverse transcriptases, among which *Escherichia coli* RNase HI (5, 6) and the RNase H domain of HIV-1 reverse transcriptase (7) have been most extensively studied in terms of their structures and functions. The Type 2 enzymes can be further divided into bacterial RNases HII and HIII, eukaryotic RNases H2, and archaeal RNases HIII, among which the crystal structures of some archaeal RNases HII have thus far been determined (8–10). Because these structures highly resemble one another, we selected and studied the RNase HII from *Thermococcus kodakaraensis* as a representative of the archaeal RNases HII. Despite having poor amino acid sequence similarity, *T. kodakaraensis* RNase HII (8) and *E. coli* RNase HI (11, 12)

share a main chain fold consisting of a five-stranded β -sheet and two α -helices. Also, the geometrical arrangement of the four acidic active-site residues (Asp7, Glu8, Asp105, and Asp135 for *T. kodakaraensis* RNase HII; Asp10, Glu48, Asp70 and Asp134 for *E. coli* RNase HI) is similar in these two proteins. These findings strongly suggest that the Type 1 and Type 2 enzymes share a common catalytic mechanism. According to a general acid-base mechanism proposed for *E. coli* RNase HI (5), one divalent metal cation is required for activity and the hydroxyl ion, which attacks the phosphate group for the RNA cleavage, is activated by an amino acid residue.

Because of similarities in their amino acid sequences and biochemical properties, bacterial and archaeal RNases HII are envisaged to share a common three-dimensional structure (13). However, RNases HII from mesophilic bacteria have relatively long N-terminal extensions as compared to their archaeal counterparts (4). For example, the N-terminal of *Bacillus subtilis* RNase HII, which has the longest known extension, is extended by 71 residues as compared to *T. kodakaraensis* RNase HII. In contrast, RNases HII from thermophilic bacteria, such as *Aquifex aeolicus* and *Thermotoga maritima*, do not have such long extensions. These findings may indicate that the absence of a large N-terminal extension is related to the functional adaptation of RNase HII enzymes to a thermophilic environment. Hence, it will

* Corresponding author. e-mail: kanaya@ap.chem.eng.osaka-u.ac.jp
phone/fax: +81-(0)6-6879-7938

be informative to examine whether RNases HIII from thermophilic *Bacillus* strains have an N-terminal extension similar in length to that of *B. subtilis* RNase HIII.

Bacillus stearothermophilus is a thermophilic *Bacillus* strain that grows optimally at 60°C. In the work reported here, we cloned the gene from this strain that encodes RNase HIII, expressed it in *E. coli*, and purified and biochemically characterized the overproduced protein (*Bst*-RNase HIII). We found that *Bst*-RNase HIII contains an N-terminal extension similar to that of *B. subtilis* RNase HIII. Construction and examination of a truncated protein with most of this N-terminal extension removed, followed by biochemical characterization, suggest that the N-terminal extension is important for substrate binding.

MATERIALS AND METHODS

Cells and plasmids *B. stearothermophilus* CU21 was previously isolated (14). The *rnhA* mutant strain *E. coli* MIC3009 [*F*⁻, *supE44*, *supF58*, *lacY1* or Δ (*lacIZY*)6, *trpR55*, *galK2*, *galT22*, *metB1*, *hsdR14*($r_K^-m_K^-$), *rnhA339::cat*] (15) was kindly donated by M. Itaya. Competent cells of *E. coli* HB101 [*F*⁻, *hsdS20*($r_B^-m_B^-$), *recA13*, *ara-13*, *proA2*, *lacY1*, *galK2*, *rpsL20*(Sm^r), *xyl-5*, *mtl-1*, *supE44*, λ^-] and the plasmid pUC18 were obtained from Takara Shuzo (Kyoto). The plasmid pJLA503 was constructed by Schauder *et al.* (16). *E. coli* transformants were grown in Luria-Bertani medium containing 0.1 g/l ampicillin.

Gene cloning The genomic DNA of *B. stearothermophilus* CU21 was prepared as previously described (17) and used as a template to amplify a part of the gene (*Bst-rnhB*) encoding *Bst*-RNase HIII by PCR. The sequences of the PCR primers were 5'-GACGAGGTCGGCCGGGGGCC-3' for the 5'-primer and 5'-CGTCCCTCGTCACTTTTGC-3' for the 3'-primer. PCR was performed with the GeneAmp PCR System 2400 (Perkin-Elmer, Tokyo) using a KOD polymerase (Toyobo, Kyoto) according to the procedures recommended by the supplier. The amplified DNA fragment was used as a probe for Southern blotting and colony hybridization to clone the entire *Bst-rnhB* gene. These procedures were carried out using the AlkPhos Direct system (Amersham Pharmacia Biotech, Tokyo) as recommended by the supplier. The DNA sequence was determined by a Prism 310 DNA sequencer (Perkin-Elmer).

Plasmid construction The cloned *Bst-rnhB* gene was amplified by PCR performed twice using a 5'-primer (5'-AGGGAGAG ACATATGAAGGAGTA-CACG-3'), 3'-primer (5'-GCGTCCGACTGTCCGCTTGA CTGCCTGCA-3'), 5'-mutagenic primer (5'-GC CCGCCACATGGGTAC-3'), and 3'-mutagenic primer (5'-GTAA CCCATGTGGCGGGC-3'), as described previously for the construction of mutant *E. coli* RNase HI proteins (18). In the above sequences, underlined bases show the positions of the *NdeI* (5'-primer) and *SalI* (3'-primer) sites. The 5'-mutagenic primer, which is complementary to the 3'-mutagenic primer, was designed to silently eliminate the *NdeI* site encompassing the sequences coding for His²²³-Met²²⁴. After digestion by *NdeI* and *SalI*, the PCR fragment was ligated into the *NdeI*-*SalI* sites of plasmid pJLA503 to generate plasmid pJAL800ST, in which the transcription of the *Bst-rnhB* gene is controlled by the bacteriophage λ P_L and P_R promoters.

The truncated *Bst-rnhB* gene, encoding Δ 59-*Bst*-RNase HIII in which 59 N-terminal residues are removed, was constructed by PCR using a 5'-primer (5'-GTTGGGAGGAGCATATGCGCTATGAGCGTG-3': the underlined bases show the position of the *NdeI* site) and the 3'-primer mentioned above. Plasmid pJAL800ST was used as a template. After digestion by *NdeI* and *SalI*, the PCR frag-

ment was ligated into the *NdeI*-*SalI* sites of plasmid JLA503 to generate plasmid pJAL680ST.

Overproduction and purification Overproducing strains were constructed by transforming *E. coli* MIC3009 with pJAL800ST or pJAL680ST. Overproduction was achieved by shifting the cultivation temperature from 30°C to 42°C in the logarithmic growth phase, as described previously for *E. coli* RNase HI (19). Cells were then harvested by centrifugation at 5000×g for 10 min and purified as follows.

Bst-RNase HIII and Δ 59-*Bst*-RNase HIII were purified from *E. coli* MIC3009 cells transformed with pJAL800ST and pJAL680ST, respectively, by identical procedures, which were all carried out at 4°C. Cells were suspended in 10 mM Tris-HCl (pH 7.5) containing 1 mM EDTA (TE-buffer), disrupted by sonication with a sonifier (model 450; Branson Ultrasonic, Danbury, CT, USA), and centrifuged at 30,000×g for 30 min. The supernatant was pooled and fractionated with ammonium sulfate precipitation. The precipitates obtained at 30–60% saturation of ammonium sulfate were collected by centrifugation at 10,000×g for 20 min and dissolved in TE-buffer. The resultant solution was dialyzed against the same buffer and applied to a column of Hitrap Q (Amersham Pharmacia Biotech, Piscataway, NJ, USA) equilibrated with the same buffer. The pass-through fraction was applied to a column of Hitrap heparin (Amersham Pharmacia Biotech) equilibrated with the same buffer. The enzyme was eluted from the column at an NaCl concentration of 0.3 M by linearly increasing the NaCl concentration from 0 to 0.5 M. The fractions containing the enzyme were combined and used for further analyses. The purity of the enzyme was analyzed by SDS-PAGE on a 12% polyacrylamide gel (20), followed by staining with Coomassie brilliant blue R250.

Biochemical characterization The molecular mass of the protein was estimated by gel filtration chromatography using a column (1.6×60 cm) of Superdex 200 (Amersham Pharmacia Biotech) equilibrated with 10 mM Tris-HCl (pH 7.5) containing 150 mM NaCl. Bovine serum albumin (67 kDa), ovalbumin (43 kDa), chymotrypsinogen A (25 kDa), and RNase A (13.7 kDa) were used as standard proteins.

The far-UV CD spectra were measured at 30°C in 50 mM Tris-HCl (pH 8.0) on an automatic spectropolarimeter (J725; Japan Spectroscopic, Tokyo). The protein concentration was ~0.1 mg/ml and a cell with an optical path of 2 mm was used. The mean residue ellipticity, θ (deg cm² dmol⁻¹), was calculated using an average amino acid molecular mass of 110 Da.

Enzymatic activity The RNase H activity was determined at 30°C for 15 min in 10 mM Tris-HCl (pH 8.0) containing 10 mM MnCl₂, 50 mM NaCl, 1 mM 2-mercaptoethanol, and 10 μg/ml bovine serum albumin, by measuring the radioactivity of the acid-soluble digestion product from the substrate, a ³H-labeled M13 DNA/RNA hybrid, as previously described (21). One unit was defined as the amount of enzyme producing 1 nmol of acid-soluble material per min at 30°C. The specific activity was defined as the enzymatic activity per mg of protein. The protein concentration was determined from the UV absorption with A₂₈₀^{0.1%} values of 0.91 for *Bst*-RNase HIII and 0.66 for Δ 59-*Bst*-RNase HIII. These values were calculated by using ϵ values of 1576 M⁻¹ cm⁻¹ for Tyr and 5225 M⁻¹ cm⁻¹ for Trp at 280 nm (22).

Binding analysis Interaction between the protein and substrate was analyzed with a BIAcore instrument (Biacore, Tokyo) using a sensor chip on which a 36-bp DNA/RNA hybrid was immobilized, as described previously (23). The sensorgrams were analyzed using BIAevaluation software (Biacore) to estimate the association constant K_A.

3D modeling The amino acid sequences of *Bst*-RNase HIII and *T. kodakaraensis* RNase HIII were aligned based on the secondary structures of *Bst*-RNase HIII predicted by the EMBL PredictProtein server. This alignment and the coordinates from the

crystal structure of the *T. kodakaraensis* RNase HII were used to build a 3D model of *Bst*-RNase HII by satisfying spatial restraints (24–28) using the Modeller-4 program. Energy minimization and simulated annealing were carried out with the CNSsolve package version 1.0 (29). The stereochemistry and geometry of the model at all stages of refinement were checked using the PROCHECK program (30).

RESULTS AND DISCUSSION

Cloning of the *Bst-rnhB* gene When the amino acid sequences of various bacterial RNases HII are compared, the sequences DEVGRGP and AKVTRDR, which respectively correspond to Asp⁷⁸-Pro⁸⁴ and Ala²⁰⁰-Arg²⁰⁶ of *B. subtilis* RNase HII, are observed to be highly conserved (4). On the assumption that the nucleotide sequence of the *B. subtilis* RNase HII gene is conserved in the *Bst-rnhB* gene in the regions where the amino acid sequences are conserved, DNA oligomers with the sequences encoding Asp⁷⁸-Pro⁸⁴ and Ala²⁰⁰-Arg²⁰⁶ of *B. subtilis* RNase HII were synthesized and used to amplify a part of the *Bst-rnhB* gene. PCR using the genomic DNA of *B. stearothermophilus* CU21 as a template produced only a 386-bp DNA fragment encoding a part of the *Bst*-RNase HII sequence. Southern blotting and colony hybridization using this DNA fragment as a probe indicated that a 2.0-kb *Bam*HI fragment of the CU21 genome contains the entire *Bst-rnhB* gene (data not shown). Determination of the nucleotide sequence of the *Bst-rnhB* gene revealed that *Bst*-RNase HII is composed of 259 amino acid residues with a calculated molecular mass of 28,892 Da and an isoelectric point of 8.6. A potential Shine-Dalgarno (SD) sequence (5'-GGAG-3'), which is complementary to the 3'-terminal sequence of 16S rRNA from CU21, is located six nucleotides upstream of the initiation codon for translation. The nucleotide sequence of the *Bst-rnhB* gene has been deposited in DDBJ with accession number AB073670.

Comparison of amino acid sequences The amino acid sequence of *Bst*-RNase HII deduced from the nucleotide sequence showed the highest identity (50.2%) to *B. subtilis* RNase HII. In Fig. 1, these sequences, as well as the amino acid sequences of RNases HII from *Methanococcus jannaschii* and *T. kodakaraensis*, for which the crystallographic structures are available, are aligned based on the elements of their secondary structures. Both *Bst*-RNase HII and *B. subtilis* RNase HII have a 71-residue extension at the N-terminus, as compared to the sequences of *M. jannaschii* and *T. kodakaraensis* RNases HII. Without this N-terminal extension, *Bst*-RNase HII would have amino acid sequence identities of 26.0% to *M. jannaschii* RNase HII and 29.8% to *T. kodakaraensis* RNase HII. The four acidic amino acid residues involved in divalent cation binding and catalytic function, which are fully conserved in the various RNase HII sequences, are also conserved in the *Bst*-RNase HII sequence. These residues are Asp⁷⁸, Glu⁷⁹, Asp¹⁷⁰, and Asp¹⁸⁷. In addition, several conserved sequence motifs, such as GRGP and DSK, are conserved in the *Bst*-RNase HII sequence. These features suggest that *Bst*-RNase HII resembles other RNases HII both structurally and functionally.

Biochemical properties of recombinant *Bst*-RNase HII

Upon induction, *Bst*-RNase HII accumulated in *E. coli* cells in a soluble form. Its production level was roughly 5 mg/l culture. The protein was purified to give a single band on SDS-PAGE with a yield of ~20% (data not shown). The molecular mass of the protein was estimated to be 31 kDa by both SDS-PAGE and gel filtration column chromatography, which is comparable to the calculated value. These results strongly suggest that like *B. subtilis* (3) and *T. kodakaraensis* (31) RNases HII, *Bst*-RNase HII exists in a monomeric form.

Bst-RNase HII requires a divalent metal cation for activity. Like *B. subtilis* (3) and *E. coli* (32) RNases HII, it prefers Mn²⁺ to Mg²⁺, and shows the highest RNase H activity at pH 8 in the presence of 10 mM MnCl₂ and 50 mM NaCl. The temperature dependence of the *Bst*-RNase HII activity was not analyzed because the substrate is unstable at high temperatures. The specific activity of *Bst*-RNase HII was determined to be 20±4 units/mg at 30°C (average of values obtained from two independent experiments), which is 25- and 15-fold lower than those of *B. subtilis* and *E. coli* RNases HII, respectively.

When *Bst*-RNase HII and *B. subtilis* RNase HII (0.1 mg/ml) were incubated at various temperatures for 10 min in 10 mM Tris-HCl (pH 7.5) containing 1 mM EDTA, 0.1 M NaCl, and 10% glycerol and the residual activities were determined at 30°C, *Bst*-RNase HII and *B. subtilis* RNase HII lost half their activity at incubation temperatures of ~60°C and ~40°C, respectively. These results suggest that the thermostability of *Bst*-RNase HII is higher than that of *B. subtilis* RNase HII. Thus, an absence of long N-terminal extensions in the amino acid sequences of RNases HII from thermophilic sources seems to be unrelated to the adaptation of these enzymes to high temperatures. The factors that make *Bst*-RNase HII more stable than *B. subtilis* RNase HII remain to be determined.

Properties of Δ59-*Bst*-RNase HII By analyzing the biochemical properties of truncated proteins of *T. kodakaraensis* RNase HII in which 15, 21, 25, and 30 residues were removed from the C-terminus, it has previously been shown that the α9 helix of this enzyme is important for substrate binding (8). Because this helix is rich in basic amino acid residues, it may bind to the negatively charged DNA/RNA substrate through electrostatic interaction. However, *Bst*-RNase HII lacks most of the amino acid residues that form this helix. The question thus arises as to whether *Bst*-RNase HII possesses an alternative substrate binding domain. Because basic amino acid residues are clustered at positions 41–55 within the N-terminal extension of *Bst*-RNase HII, it was thought that this extension may function as a substrate binding domain in this protein. To verify whether this is the case, the truncated protein Δ59-*Bst*-RNase HII, in which 59 N-terminal residues were removed, was constructed and its biochemical properties were analyzed. This truncated protein was overproduced in *E. coli* cells and purified to give a single band on SDS-PAGE, as was the intact protein. The truncated and intact proteins gave almost identical far-UV CD spectra (data not shown), suggesting that the protein conformation was not seriously changed upon N-terminal truncation. Nevertheless, Δ59-*Bst*-RNase HII completely lost

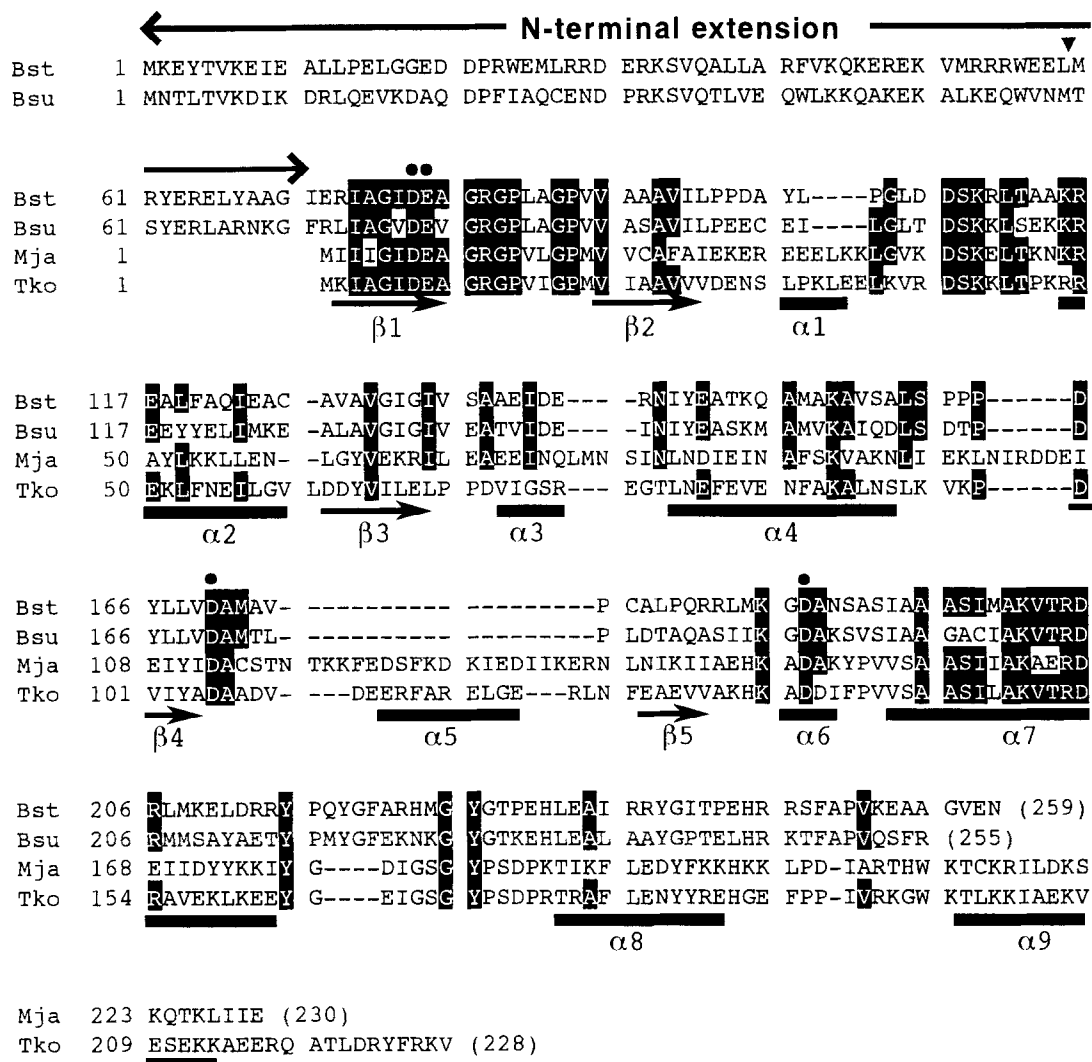


FIG. 1. Alignment of amino acid sequences of RNases HII. The amino acid sequence of *Bst*-RNase HII (Bst) is compared with those of RNases HII from *B. subtilis* (Bsu) (genome data bank entry: Bsu:rnh), *M. jannaschii* (Mja) (GenBank, U67470), and *T. kodakaraensis* KOD1 (Tko) (DDBJ, AB012613). Gaps are denoted by dashes. Amino acid residues conserved in at least three different enzymes are shown by white letters on a black background. The four acidic catalytic residues are marked by black circles. Numbers indicate the positions of the amino acid residues, which start from the initiator methionine for each enzyme. The ranges of the nine α -helices and five β -strands of *T. kodakaraensis* (8) and *M. jannaschii* (9) RNases HII are shown below the sequences. The position at which the N-terminal extension is truncated to create $\Delta 59$ -*Bst*-RNase HII is indicated by a black inverted triangle.

its RNase H activity.

To examine whether N-terminal truncation seriously affects substrate-binding affinity, interaction between the protein and substrate was analyzed using surface plasmon resonance. The sensorgrams obtained for the interaction between the intact protein and the substrate are shown in Fig. 2A. The responses increased with increasing protein concentration. From the plot of RU_{eq}/C as a function of RU_{eq} shown in Fig. 2B, the association constant K_A was estimated to be $(2.15 \pm 0.43) \times 10^7$ (mean \pm S.E., $n=7$). In contrast, the sensorgrams for the interaction between the truncated protein and the substrate did not give such positive signals. The response did not increase beyond the background level at any protein concentration examined, indicating that $\Delta 59$ -*Bst*-RNase HII does not bind to the substrate. These results suggest that the N-terminal extension of *Bst*-RNase HII is

important for substrate binding.

Substrate binding domain *T. kodakaraensis* RNase HII and *E. coli* RNase HI share a main chain fold termed the "RNase H fold" (8). This fold is conserved in all members of nucleotidyltransferase superfamilies (33). However, these two enzymes differ in the location of the domain involved in substrate binding. In *T. kodakaraensis* RNase HII, it occurs as an extra C-terminal domain (8) whereas in *E. coli* RNase HI it is as an internal domain termed the "basic protrusion" (34). Our findings indicate that *Bst*-RNase HII may represent a novel type of RNase H that differs from *T. kodakaraensis* RNase HII and *E. coli* RNase HI in its substrate binding domain location. Because the N-terminal extension of bacterial RNases HII differ greatly in length, it remains to be determined whether other bacterial RNases HII, including that of *E. coli*, also have a substrate binding

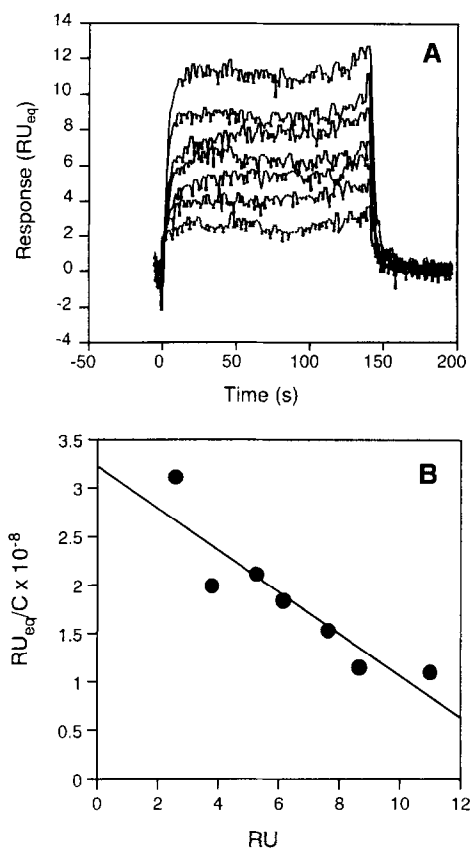


FIG. 2. BIAcore analysis of interaction between the protein and substrate. (A) Sensorgrams for the interaction between *Bst*-RNase HII and the 36-bp DNA/RNA hybrid. The protein was dissolved in 10 mM Tris-HCl (pH 8.0) containing 50 mM NaCl, 1 mM EDTA, 1 mM 2-mercaptoethanol, and 0.005% Tween P20 at concentrations ranging from 10 to 100 nM. The sample was injected at 25°C with a flow rate of 30 μ l/min onto the surface of the sensor chip on which the 36-bp DNA/RNA hybrid was immobilized. (B) Plot for determining the equilibrium association constant K_A using equilibrium sensor responses (RU_{eq}). The RU_{eq}/C values were plotted versus the RU_{eq} values shown in (A). Linear transformation of the plot gives the association constant K_A .

domain at their N-termini. In contrast, none of the amino acid sequences of archaeal RNases HII so far available contain an N-terminal extension, suggesting that archaeal RNases HII possess a substrate binding domain at their C-termini. To understand the role of the N-terminal extensions of *Bacillus* RNases HII, it will be necessary to determine their crystal structures.

3D modeling The fact that the amino acid sequence of *Bst*-RNase HII at the core region does not contain large insertions when compared to that of *T. kodakaraensis* RNase HII (Fig. 1) allowed us to build a model of the three-dimensional structure of the *Bst*-RNase HII core region. Comparison of this 3D-model with the crystal structure of *T. kodakaraensis* RNase HII suggests that the *Bst*-RNase HII structure is similar to that of *T. kodakaraensis* RNase HII (Fig. 3). The steric configurations of the four acidic catalytic residues are well conserved in the two structures. However, the former lacks the $\alpha 5$ helix and most of the $\alpha 9$ helix. This difference reflects the large internal deletion and C-terminal truncation in the amino acid sequence of *Bst*-

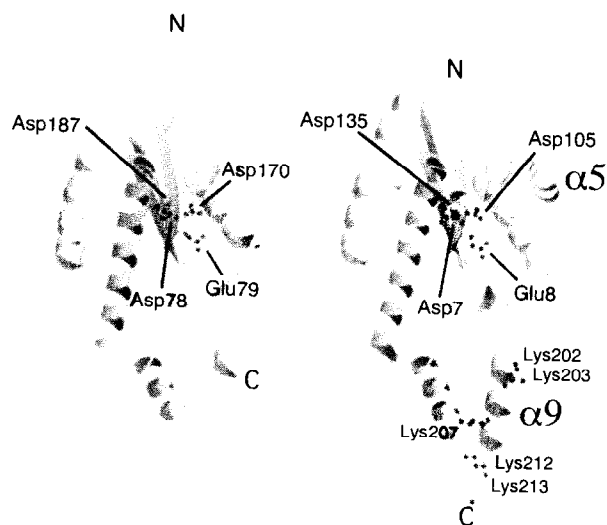


FIG. 3. Schematic depictions of 3D-model of *Bst*-RNase HII (left) and crystal structure of *T. kodakaraensis* RNase HII (right). N and C represent the N- and C-termini of the proteins. The side chains of the four fully conserved acidic residues that have been shown to be required for activity of *T. kodakaraensis* RNase HII (8), as well as those of the five basic residues, which are located in the $\alpha 9$ -helix of *T. kodakaraensis* RNase HII and envisaged to be involved in substrate binding (8), are indicated. The broken line represents the N-terminal extension of *Bst*-RNase HII. The positions of the $\alpha 5$ and $\alpha 9$ helices, which are absent or mostly absent in the *Bst*-RNase HII structure, are indicated. The structures were drawn with Molscript and Raster3D.

RNase HII (Fig. 1).

According to the crystal structure of *T. kodakaraensis* RNase HII, the $\alpha 5$ helix is located in the vicinity of a catalytic site and forms a hydrophobic core with a central β -sheet (Fig. 3). Because bacterial RNases HII prefer Mn^{2+} to Mg^{2+} for activity (13), whereas *T. kodakaraensis* RNase HII exhibits its activity almost equally in the presence of Mn^{2+} and Mg^{2+} , this helix may be related to the metal ion preference of the enzyme.

REFERENCES

1. Crouch, R. J. and Dirksen, M.-L.: Ribonuclease H, p. 211–241. In Linn, S. M. and Roberts, R. J. (ed.), *Nucleases*. Cold Spring Harbor Laboratory, Cold Spring Harbor, NY (1982).
2. Kogoma, T. and Foster, P. L.: Physiological functions of *E. coli* RNase HI, p. 39–66. In Crouch, R. J. and Toulme, J. J. (ed.), *Ribonucleases H*. INSERM, Paris (1998).
3. Ohtani, N., Haruki, M., Morikawa, M., Crouch, R. J., Itaya, M., and Kanaya, S.: Identification of the genes encoding Mn^{2+} -dependent RNase HII and Mg^{2+} -dependent RNase HIII from *Bacillus subtilis*: Classification of RNases H into three families. *Biochemistry*, **38**, 605–618 (1999).
4. Ohtani, N., Haruki, M., Morikawa, M., and Kanaya, S.: Molecular diversities of RNases H. *J. Biosci. Bioeng.*, **88**, 12–19 (1999).
5. Kanaya, S.: Enzymatic activity and protein stability of *E. coli* ribonuclease HI, p. 1–38. In Crouch, R. J. and Toulme, J. J. (ed.), *Ribonucleases H*. INSERM, Paris (1998).
6. Kanaya, S. and Ikehara, M.: Functions and structures of ribonuclease H enzymes, p. 377–422. In Biswas, B. B. and Roy, S. (ed.), *Subcellular biochemistry*, vol. 24: proteins: structure, function, and engineering. Plenum Press, New York (1995).

7. **Hughes, S. H., Arnold, E., and Hostomsky, Z.:** RNase H of retroviral reverse transcriptase, p.195–224. In Crouch, R. J. and Toulme, J. J. (ed.), *Ribonucleases H*. INSERM, Paris (1998).
8. **Muroya, A., Tsuchiya, D., Ishikawa, M., Haruki, M., Morikawa, M., Kanaya, S., and Morikawa, K.:** Catalytic center of an archaeal type 2 ribonuclease H as revealed by X-ray crystallographic and mutational analyses. *Protein Sci.*, **10**, 707–714 (2001).
9. **Lai, L., Yokota, H., Hung, L. W., Kim, R., and Kim, S. H.:** Crystal structure of archaeal RNase HII: a homologue of human major RNase H. *Structure*, **8**, 897–904 (2000).
10. **Chapados, B. R., Chai, Q., Hosfield, D. J., Shen, B., and Tainer, J. A.:** Structural biochemistry of a type 2 RNase H: RNA primer recognition and removal during DNA replication. *J. Mol. Biol.*, **307**, 541–556 (2001).
11. **Katayanagi, K., Miyagawa, M., Matsushima, M., Ishikawa, M., Kanaya, S., Ikehara, M., Matsuzaki, T., and Morikawa, K.:** Three-dimensional structure of ribonuclease H from *E. coli*. *Nature*, **347**, 306–309 (1990).
12. **Yang, W., Hendrickson, W. A., Crouch, R. J., and Satow, Y.:** Structure of ribonuclease H phased at 2 Å resolution by MAD analysis of the selenomethionyl protein. *Science*, **249**, 1398–1405 (1990).
13. **Kanaya, S.:** Prokaryotic type 2 RNases H. *Methods Enzymol.*, **341**, 377–394 (2001).
14. **Imanaka, T., Fujii, M., Aramori, I., and Aiba, S.:** Transformation of *Bacillus stearothermophilus* with plasmid DNA and characterization of shuttle vector plasmids between *Bacillus stearothermophilus* and *Bacillus subtilis*. *J. Bacteriol.*, **149**, 824–830 (1982).
15. **Itaya, M. and Crouch, R. J.:** A combination of RNase H (*rnh*) and *rec BCD* or *sbcb* mutations in *Escherichia coli* K12 adversely affects growth. *Mol. Gen. Genet.*, **227**, 424–432 (1991).
16. **Schauder, B., Blocker, H., Frank, R., and McCarthy, J. E.:** Inducible expression vectors incorporating the *Escherichia coli atpE* translational initiation region. *Gene*, **52**, 279–283 (1987).
17. **Imanaka, T., Tanaka, T., Tsunekawa, H., and Aiba, S.:** Cloning of the genes for penicillinase, *penP* and *penI*, of *Bacillus licheniformis* in some vector plasmids and their expression in *Escherichia coli*, *Bacillus subtilis*, and *Bacillus licheniformis*. *J. Bacteriol.*, **147**, 776–786 (1981).
18. **Kanaya, S., Oobatake, M., Nakamura, H., and Ikehara, M.:** pH-dependent thermostabilization of *Escherichia coli* ribonuclease HI by histidine to alanine substitutions. *J. Biotechnol.*, **28**, 117–136 (1993).
19. **Kanaya, S., Kohara, A., Miyagawa, M., Matsuzaki, T., Morikawa, K., and Ikehara, M.:** Overproduction and preliminary crystallographic study of ribonuclease H from *Escherichia coli*. *J. Biol. Chem.*, **264**, 11546–11549 (1989).
20. **Laemmli, U. K.:** Cleavage of structural proteins during the assembly of the head of bacteriophage T4. *Nature*, **227**, 680–685 (1970).
21. **Kanaya, S., Katsuda, C., Kimura, S., Nakai, T., Kitakuni, E., Nakamura, H., Katayanagi, K., Morikawa, K., and Ikehara, M.:** Stabilization of *Escherichia coli* ribonuclease H by introduction of an artificial disulfide bond. *J. Biol. Chem.*, **266**, 6038–6044 (1991).
22. **Goodwin, T. W. and Morton, R. A.:** The spectrophotometric determination of tyrosine and tryptophan in proteins. *Biochem. J.*, **40**, 628–632 (1946).
23. **Haruki, M., Noguchi, E., Kanaya, S., and Crouch, R. J.:** Kinetic and stoichiometric analysis for the binding of *Escherichia coli* ribonuclease HI to RNA-DNA hybrids using surface plasmon resonance. *J. Biol. Chem.*, **272**, 22015–22022 (1997).
24. **Sali, A. and Blundell, T. L.:** Comparative protein modelling by satisfaction of spatial restraints. *J. Mol. Biol.*, **234**, 779–815 (1993).
25. **Sali, A. and Overington, J. P.:** Derivation of rules for comparative protein modeling from a database of protein structure alignments. *Protein Sci.*, **3**, 1582–1596 (1994).
26. **Sali, A., Potterton, L., Yuan, F., van Vlijmen, H., and Karplus, M.:** Evaluation of comparative protein modeling by MODELLER. *Proteins*, **23**, 318–326 (1995).
27. **Sali, A.:** Comparative protein modeling by satisfaction of spatial restraints. *Mol. Med. Today*, **1**, 270–277 (1995).
28. **Sanchez, R. and Sali, A.:** Evaluation of comparative protein structure modeling by MODELLER-3. *Proteins Suppl.*, **1**, 50–58 (1997).
29. **Brunger, A. T., Adams, P. D., Clore, G. M., DeLano, W. L., Gros, P., Grosse-Kunstleve, R. W., Jiang, J. S., Kuszewski, J., Nilges, M., Pannu, N. S. et al.:** Crystallography and NMR system (CNS): a new software suite for macromolecular structure determination. *Acta Cryst.*, **D54**, 905–921 (1998).
30. **Laskowski, R. A., MacArthur, M. W., Moss, D. S., and Thornton, J. M.:** PROCHECK: a program to check the stereochemical quality of protein structures. *J. Appl. Crystallogr.*, **26**, 283–291 (1993).
31. **Haruki, M., Hayashi, K., Kochi, T., Muroya, A., Koga, Y., Morikawa, M., Imanaka, T., and Kanaya, S.:** Gene cloning and characterization of recombinant ribonuclease HII from a hyperthermophilic archaeon. *J. Bacteriol.*, **180**, 6207–6214 (1998).
32. **Ohtani, N., Haruki, M., Muroya, A., Morikawa, M., and Kanaya, S.:** Characterization of ribonuclease HII from *Escherichia coli* overproduced in a soluble form. *J. Biochem.*, **127**, 895–899 (2000).
33. **Yang, W. and Steitz, T.:** Recombining the structures of HIV integrase, RuvC and RNase H. *Structure*, **3**, 131–134 (1995).
34. **Kanaya, S., Katsuda-Nakai, C., and Ikehara, M.:** Importance of the positive charge cluster in *Escherichia coli* ribonuclease HI for the effective binding of the substrate. *J. Biol. Chem.*, **266**, 11621–11627 (1991).